Unlocking the Mechanisms of Cutaneous Adverse Drug Reactions: Activation of the Phosphatidylinositol 3-Kinase/Protein Kinase B Pathway by EGFR Inhibitors Triggers Keratinocyte Differentiation and Polarization of Epidermal Immune Responses

Thomas Ondet[1], Pierre-François Roux[1], Mario Monshouwer[2] and Georgios N. Stamatas[1]

EGFR inhibitors used in oncology therapy modify the keratinocyte differentiation processes, impairing proper skin barrier formation and leading to cutaneous adverse drug reactions. To uncover the molecular signatures associated with cutaneous adverse drug reactions, we applied phosphoproteomic and transcriptomic assays on reconstructed human epidermis tissues exposed to a therapeutically relevant concentration of afatinib, a second-generation EGFR inhibitor. After drug exposure, we observed activation of the phosphatidylinositol 3-kinase/protein kinase B pathway associated with an increased expression of gene families involved in keratinocyte differentiation, senescence, oxidative stress, and alterations in the epidermal immune-related markers. Furthermore, our results show that afatinib may interfere with vitamin D3 metabolism, acting via CYP27A1 and CYP24A1 to regulate calcium concentration through the phosphatidylinositol 3-kinase/protein kinase B pathway. Consequently, basal layer keratinocytes switch from a pro-proliferating to a prodifferentiative program, characterized by upregulation of biomarkers associated with increased keratinization, cornification, T helper type 2 response, and decreased innate immunity. Such effects may increase skin susceptibility to cutaneous penetration of irritants and pathogens. Taken together, these findings demonstrate a molecular mechanism of EGFR inhibitor–induced cutaneous adverse drug reactions.

JID Innovations (2021);**1:**100009 doi:10.1016/j.xjidi.2021.100009

INTRODUCTION

Skin is the first line of defense against irritant, allergen, and microbial penetration, and consequently, its barrier function plays a pivotal role in the pathogenesis of cutaneous adverse drug reactions (CADRs). Under normal conditions, EGFR signaling is dominated by progrowth and prosurvival pathways (Ali et al., 2018). During oncotherapy, particularly when the target involves key drivers of keratinocyte (KC) proliferation and survival, such as EGFR (Eckert et al., 2002), the epidermis is directly impacted and undergoes alterations related to its immune function and structural integrity (Lacouture, 2006).

Afatinib (AFA), a second-generation EGFR inhibitor (EGFRi) designed to overcome resistance after therapy with first-generation drugs, was developed to irreversibly inhibit both the EGFR and HER2 signaling pathways (Li et al., 2008). Even though the mechanism of drug-induced EGFR inhibition is largely understood, the mechanism resulting in the emergence of CADRs remains unclear. Several attempts have been made so far (Peus et al., 1997), including mouse models (Lichtenberger et al., 2013; Mascia et al., 2003), but they failed to provide a complete mechanistic explanation of the molecular pathway leading to immune cell infiltration in lesional skin.

A candidate pathway for the survival of differentiating KCs is the signaling pathway that combines phosphatidylinositol 3-kinases (PI3Ks), a family of intracellular signal transducers with lipid kinase activity (Whitman et al., 1988), and the downstream serine-threonine kinase protein kinase B (Akt) effectors. The PI3K/Akt complex elicits various cell responses involving cell growth, proliferation, differentiation, and cell survival by controlling the anti-apoptotic mechanism (Calautti et al., 2005; Vivanco and Sawyers, 2002). Downstream regulation of the PI3K/Akt pathway is mediated by

[1]*SkinCare R&D, Johnson & Johnson Santé Beauté France, Issy-les-Moulineaux, France;* and [2]*Discovery Sciences, Janssen Pharmaceutical Research and Development, Beerse, Belgium*

Correspondence: Georgios N. Stamatas, SkinCare R&D, Johnson & Johnson Santé Beauté France, 1, rue Camille Desmoulins, Issy-les-Moulineaux 92787, France. E-mail: gstamata@its.jnj.com

Abbreviations: 1,25(OH)2VD3, 1,25-dihydroxyvitamine D3; AFA, afatinib; Akt, protein kinase B; C, cluster; CADR, cutaneous adverse drug reaction; CYP, cytochrome P450; EGFRi, EGFR inhibitor; K, keratin; KC, keratinocyte; LCE, late cornified envelope; PI3K, phosphatidylinositol 3-kinase; RHE, reconstructed human epidermis; Th, T helper type; TKI, tyrosine kinase inhibitor; VD3, vitamin D3

Received 19 November 2020; revised 15 February 2021; accepted 16 February 2021; accepted manuscript published online 6 March 2021; corrected proof published online 20 April 2021

Cite this article as: JID Innovations 2021;1:100009

several proteins, including the tumor suppressor PTEN (Ali et al., 2018) and caspase-3 (Jänicke et al., 1998), that drive KC differentiation and eventual cornification rather than driving their apoptosis (Lippens et al., 2005). Other proteins, including the cyclin-dependent kinase inhibitor 1, retard cell growth and promote differentiation (Missero et al., 1996).

Another candidate pathway involves vitamin D3 (VD3) or cholecalciferol, which is a factor that is often overlooked despite its critical role in epidermal development. VD3 is a secosteroid hormone synthesized in KCs through UVB-induced photolysis via synthesis of 7-dehydrocholesterol, which results in the formation of precursor VD3. The latter is then enzymatically hydroxylated to calcidiol by CYP, more specifically CYP2R1 and CYP27A1. Of note, precursor VD3 poorly regulates CYP2R1, contrary to CYP27A1, which is highly activated by precursor VD3 (Cheng et al., 2004; Mehlig et al., 2015). VD3 has a recognized impact on muscular, skeletal, and immune physiology and is capable of promoting apoptosis and epithelial differentiation (Shaurova et al., 2020). CYP27A1 is also involved in the degradation of cholesterol in bile acids through both classic and acidic pathways (Norlin et al., 2003).

We previously reported that EGFRis promote KC differentiation and reduce proliferation (Joly-Tonetti et al., 2021). However, the molecular mechanisms associated with CADRs, including skin rashes or more severe reactions, such as hand-foot syndrome or Stevens–Johnson syndrome, remain unclear. AFA, a second-generation EGFRi drug, impairs skin barrier structure by decreasing epidermal thickness, reducing KC proliferation, and increasing expression of differentiation markers such as involucrin, filaggrin, and desmoglein-1 (Joly-Tonetti et al., 2021).

To better understand the mechanism of EGFRi-induced CADRs, we assessed the consequences of AFA at a pharmaceutically relevant concentration on reconstructed human epidermis (RHE) using phosphoproteomic and transcriptomic assays.

RESULTS

Protein phosphorylation status and gene expression in RHE KCs dynamically change after exposure to EGFRi

A phospho-antibody microarray was used to identify differences in the phosphorylation status of proteins from RHE tissues after exposure to 100 nM AFA for 20 minutes, 24 hours, and 72 hours. In this assay, 1,318 proteins, including 615 phosphoproteins, were sc8reened, and changes in their phosphorylation status were recorded at each time point (Supplementary Table S1). A total of 62 phosphoproteins changed their phosphorylation status by more than 20% (Figure 1a). After exposure to AFA for 20 minutes, 24 hours, and 72 hours, the number of proteins showing increased phosphorylation compared with controls was 6, 18, and 6, respectively, and the number of proteins showing decreased phosphorylation compared with controls was 3, 23, and 6, respectively.

Unsupervised clustering was performed to categorize the proteins into clusters (Cs) depending on the level of alteration of their phosphorylation status and the timepoint when the event was detected. Such clustering allows for a more precise determination of the biological functions, interactions, or pathways that are enriched. After defining the optimal number of Cs, the proteins were grouped into two Cs, the first one (C1) representing proteins with decreased levels of phosphorylation at 24 hours and the second (C2) representing those with increased levels of phosphorylation at 24 hours (Figure 2a and b).

Transcriptomic analysis of RHE KCs treated with AFA was assessed by screening for the expression of 36,000 genes and long noncoding RNA (Supplementary Table S2). A cutoff at 50% in the fold change expression revealed the dysregulation of 2,182 genes at different time points. After 6 hours of exposure to 100 nM AFA, 170 genes were downregulated compared with controls, and 201 genes were upregulated. At 24 hours of exposure, the expression of 335 genes was decreased and the expression of 281 genes was increased. At 72 hours of exposure, the expression of 2,888 genes was decreased and the expression of 1,728 genes was increased (Figure 1b).

Unsupervised clustering was performed for the transcriptomic data to categorize the genes into clusters depending on changes in their expression levels after exposure to AFA and the timepoint when the event was detected. After defining the optimal number of Cs, the data were grouped as follows (Figure 2c and d): C1, representing early (20 minutes) downregulated genes that maintain their status at all three time points tested; C2, representing the early (20 minutes) upregulated genes that maintain their status at all three time points; C3, representing transiently upregulated genes at 24 hours; C4, representing transiently upregulated genes at 24 hours with higher amplitude than C3; C5, representing early upregulated genes followed by downregulation at 72 hours; and C6, representing downregulated genes at 24 hours followed by upregulation at 72 hours.

Protein phosphorylation array analysis demonstrates activation of the PI3K/Akt pathway with implications on cellular senescence

Based on alterations of phosphorylation status, set enrichment analysis identified the PI3K/Akt pathway as the main enriched pathway (Figure 1c) and, more specifically, the senescence pathway (Figure 1d). Upstream of PI3K, proteins with increased phosphorylation included RAC1 and FAK. Downstream of PI3K, p21 (*CDKN1*) is involved in cell cycle progression, BAD in apoptosis, and p53 in cell survival. Proteins with decreased phosphorylation are mostly inhibitors, such as PTEN, GSK3, and BCL2, and consequently promote activation of this pathway. An important number of regulated proteins downstream of the PI3K/Akt pathway are involved in cellular senescence by activating FOXO3 and the cyclin gene family (*CYCB*, *CYCD*, *CYCE*) but also the mTOR pathway and dephosphorylation of 4EBP1. The functional over-representation test showed an increased activity of proteins related to Akt phosphorylation (Figure 3a).

The transcriptomic assay results confirm activation of the PI3K/Akt pathway, as indicated by the upregulation of genes related to this pathway (C1, Figure 3b). In this case, clustering depicts dysregulation of the gene, whatever the upregulation or downregulation of the genes. In C1 (Figure 3b), the other family, negative regulation of PI3K/Akt, brings a more precise behavior of the gene family, showing that this gene's family is downregulated and consequently increases the gene associated with the PI3K/Akt pathway.

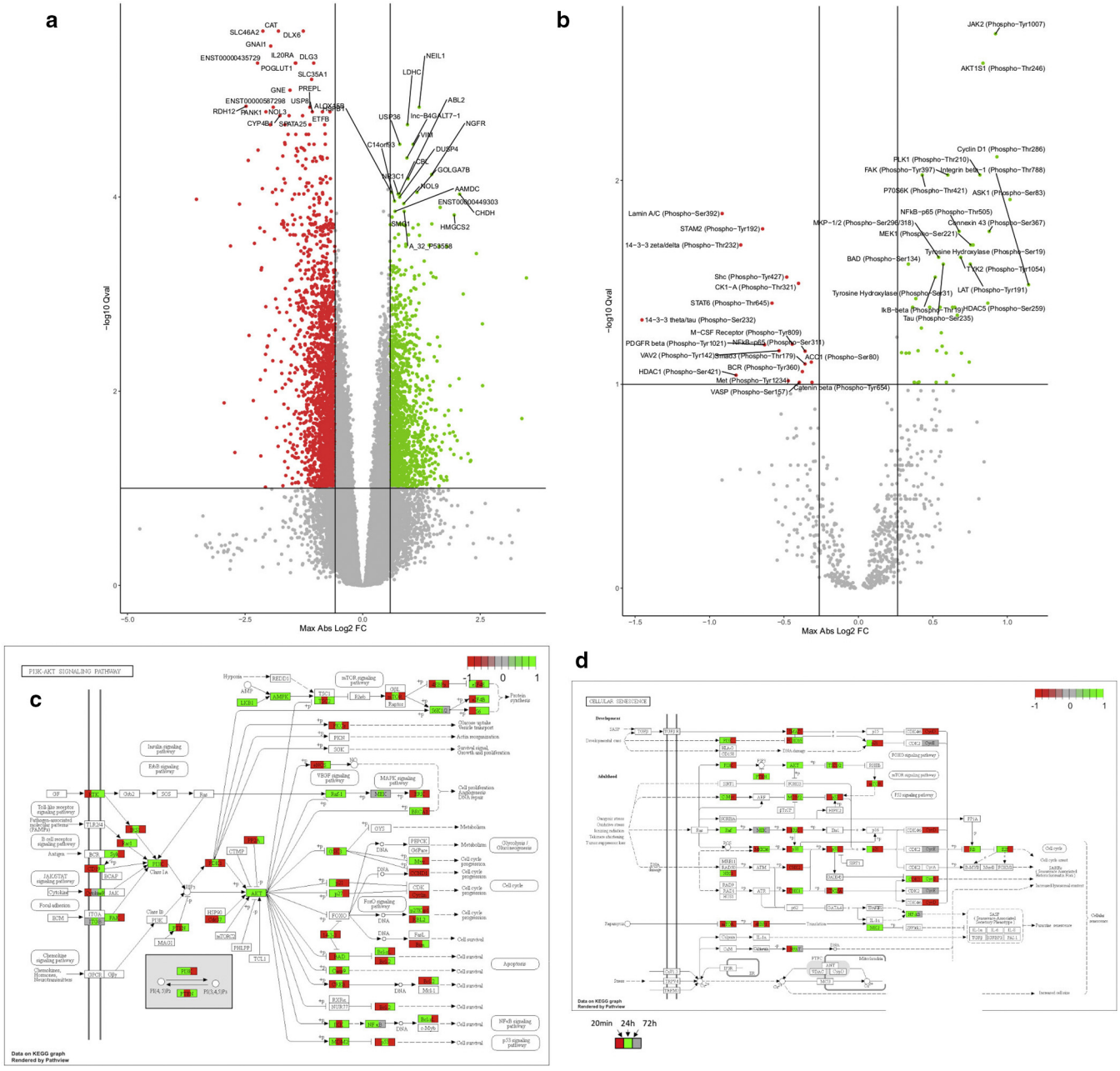

Figure 1. Functional perturbation in RHE KCs after exposure to AFA compared with Ctrl. (**a**) Generalized linear model accounting for the interaction between time and treatment was considered (afatinib at 100 nM vs. Ctrl). (**b**) Volcano plot depicting the results of the protein differential analysis performed on the phosphorylation array. Using a cutoff of 1.2-FC, 62 proteins with a change in their phosphorylation status were identified, including 44 proteins with a significant increase (green) and 18 proteins with a significant decrease (red) of their phosphorylation status. In a time-dependent manner, after 20 min of AFA exposure, the phosphorylation status of six proteins was increased and that of three proteins was decreased. At 24 h, an increased phosphorylation status was observed for 18 proteins and a decreased phosphorylation status for 23 proteins. At 72 h, the protein phosphorylation status was decreased for six proteins and increased for six others. (**c**) Volcano plot depicting the results of the differential analysis performed on gene expression (cutoff: 50%). At 6 h, the expression of 170 genes was decreased and the expression of 201 genes increased. At 24 h, 335 genes were downregulated and 281 genes upregulated. At 72 h, gene expression was increased for 2,888 genes and decreased for 1,728 genes. (**d**) SEA identified significant enrichment of the PI3K-Akt pathway at 24 h of AFA exposure. Proteins with increased phosphorylation status are shown in green and proteins with decreased phosphorylation status are shown in red. (**e**) The pathway associated with cellular senescence, involving irreversible growth arrest accompanied by phenotypic modification, showed a significant enrichment based on the change of protein phosphorylation status. The senescence pathway is downstream of the PI3K/Akt pathway. Abs, absorbance; Akt, protein kinase B; AUC, area under the curve; Ctrl, control; FC, fold change; h, hour; KC, keratinocyte; max, maximum; min, minute; PI3K, phosphatidylinositol 3-kinase; RHE, reconstructed human epidermis; SEA, set enrichment analysis.

Gene expression array analysis highlights CYP as potential oxidative stress inducer for KC differentiation

Both protein phosphorylation and gene expression arrays demonstrated that gene families involved in cellular stress, oxidative stress, and senescence were impacted after exposure to AFA (Figure 3). For example, FOXO3 phosphorylation was decreased as a consequence of PI3K/Akt pathway activation. The FOXO3 transcription factor affects

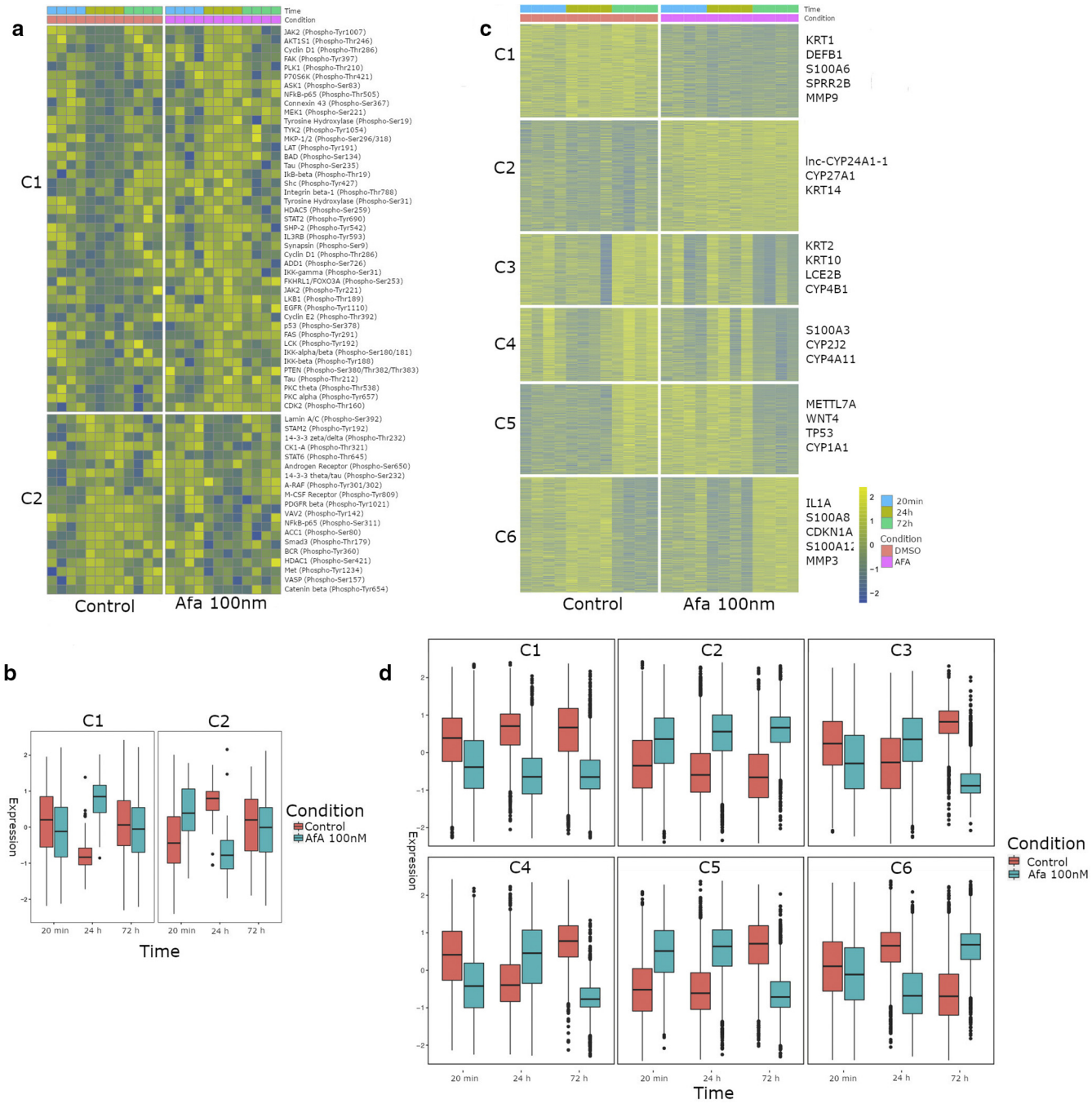

Figure 2. Clustering reveals functional impact of AFA on KC differentiation, oxidative stress, and innate immune response. (**a**) Heatmap and (**b**) boxplots depicting the results of k-means clustering based on phosphorylation status during the time-course. Data in the heatmap is expressed as row Z-score. In boxplots, the center lines depict the median; the lower and upper edges of the boxes correspond to the first and third quartiles. The upper whisker extends from the edge of the box to the largest value up to ×1.5 the IQR from the edge, and the lower whisker extends from the box edge to the smallest value at ×1.5 the IQR of the edge. (**c**) Heatmap and (**d**) boxplots depicting the results of k-means clustering based on gene expression during the time-course. Genes were divided in six clusters to classify the change in gene expression considering treatment versus control. Data in the heatmap is expressed as row Z-score. In boxplots, the center lines depict the median; the lower and upper edges of the boxes correspond to the first and third quartiles. The upper whisker extends from the edge of the box to the largest value up to ×1.5 the IQR from the edge, and the lower whisker extends from the box edge to the smallest value at ×1.5 the IQR of the edge. AFA, afatinib; C, cluster; h, hour; IQR, interquartile range; K, keratin; KC, keratinocyte; lnc, long noncoding; min, minute; MMP, matrix metalloproteinase.

cell capacity to regulate apoptosis and programmed cell death.

AFA dynamically affected the expression of genes related to oxidative stress. A large panel of metallothioneins (*MT) genes* (*MT1E*, *MT1L*, *MT1HL1*, *MT1X*, *MT1B*, *MT1A*) was decreased at 24 hours and increased at 72 hours (Figure 3b). Gene families involved in the respiratory electron transport and mitochondrial translation termination were transiently upregulated at 24 hours (Figure 3b). More specifically, the expression of the antioxidant enzymes PRDX2 and PRDX3 was decreased, and the expression of SIRT4 was increased at 72 hours (Supplementary Table S2). Of note, genes related to

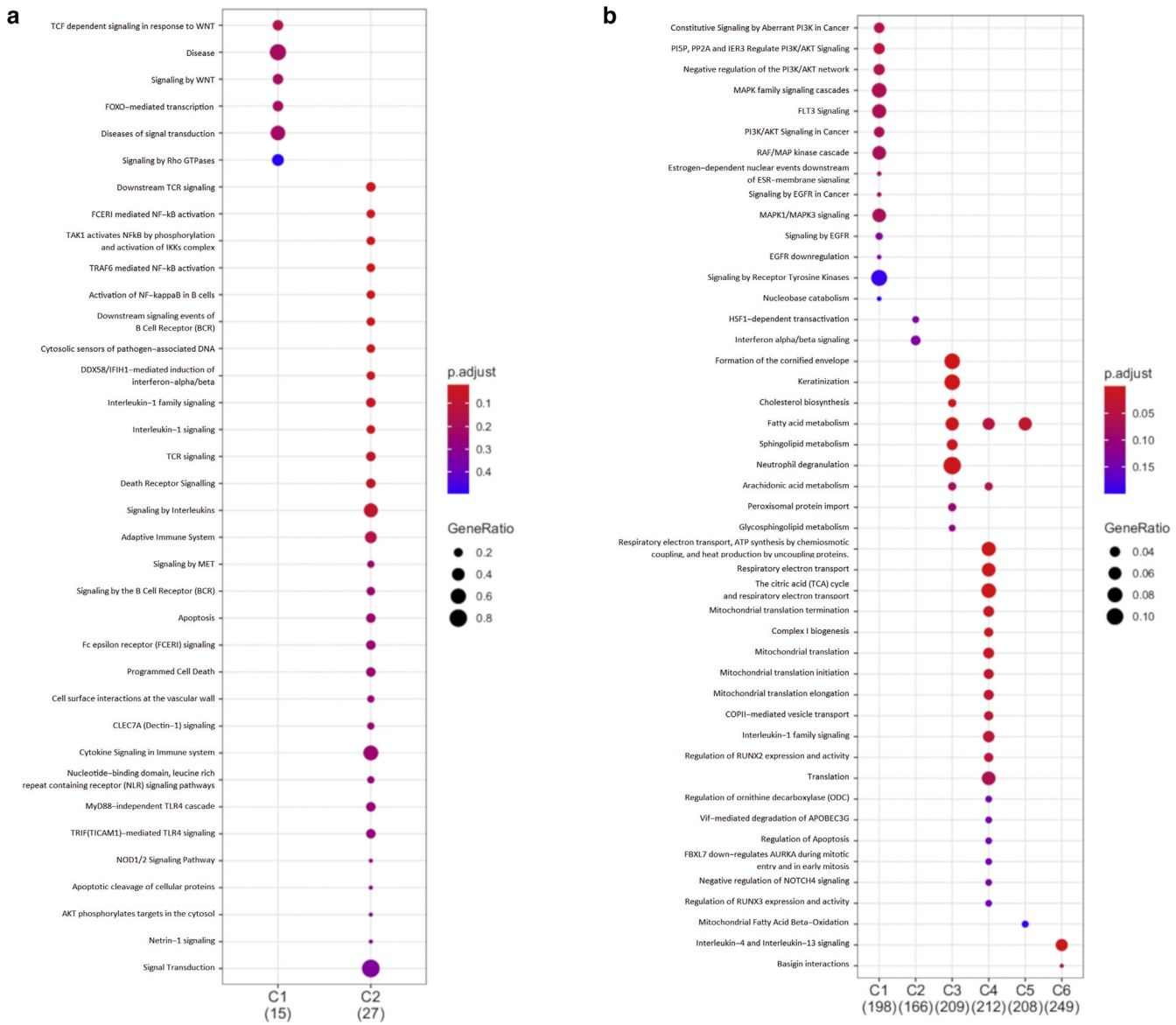

Figure 3. Over-representation analysis based on KEGG confirms functional impact of AFA on KC differentiation, oxidative stress, and innate immune response. Functional over-representation maps depicting KEGG gene sets associated with each (**a**) phosphorylation and (**b**) transcriptomic clusters. Dots are color-coded according to the FDR-corrected *P*-value based on the hypergeometric distribution. Size is proportional to the percentage of genes in the gene set belonging to the cluster. Akt, protein kinase B; ATP, adenosine triphosphate; C, cluster; FDR, false discovery rate; GTPase, guanosine triphosphatase; KC, keratinocyte; KEGG, Kyoto Encyclopedia of Genes and Genomes; ODC, ornithine decarboxylase; PI3K, phosphatidylinositol 3-kinase; TCA, tricarboxylic acid.

the metabolism of fatty acids associated with oxidative stress were first upregulated at 24 hours and then downregulated at 72 hours (Figure 3b).

We also identified changes in CYP expression at 24 hours and 72 hours. Expression of *CYP* was increased (long non-coding *CYP24A1-1*, *CYP27A1*, *CYP4F12*), and expression of other *CYP* genes was decreased (*CYP4B1*, *CYP3A7*, *CYP3A5*, *CYP2J2*, *CYP4A11*, *CYP1A1*, *CYP4F22*) (Supplementary Table S2). CYP27A1 expression could be associated with transcriptomic data involving cholesterol biosynthesis and fatty acid metabolism in C3.

Besides oxidative stress-related genes, the functional overrepresentation test (Figure 3) showed enrichment in keratinization and cornification pathways, associated with the increase at 24 hours in the expression of keratin (K) genes *K2*, *K9*, *K13*, and *K15* and late cornified envelope (LCE) genes (*LCE2A*, *LCE1B*, *LCE2B*, *LCE1C*, *LCE2D*).

Exposure to AFA perturbed the expression of innate immunity markers and enhanced the production of cytokines related to the T helper type 2 response

The PI3K/Akt pathway directly impacts both innate and adaptive epidermal immunity. Analysis of the transcriptomic data showed that genes involved in innate immunity were negatively regulated (Supplementary Table S2), including genes related to the S100 family (*S100A2*, *S100A6*, *S100A7*, *S100A8*, *S100A9*, *S100A10*, *S100A12*), *SPRR2B*, and *DEFB1* (Figure 3a).

The gene family associated with the T helper type (Th) 2 response was affected as demonstrated by over-representation

of genes related to IL-4 and IL-13 signaling (C6). These results show the kinetics of the consequences following PI3K activation, which involve activation of TCR signaling at 24 hours and, later, Th2 polarization at 72 hours.

In contrast, inflammation pathways associated with the Th1 response were barely activated. The transcriptomic data did not show any increase in expression of genes related to inflammation. The protein phosphorylation assay and the gene expression array showed a decreased inflammasome response via the toll-like receptor, NLR, and IL-1 families.

DISCUSSION

The mechanism of CADRs in patients undergoing oncotherapy remains largely unknown. The purpose of this work was to elucidate the process of EGFRi-induced CADRs at the cellular level as exemplified by those induced by AFA, a second-generation tyrosine kinase inhibitor (TKI). The majority of clinically reported skin symptoms of patients treated with small-molecule EGFRis include rashes (63% of patients), xerosis (30%), and granulomas (30%). No relationship has been reported between CADR symptoms and specific EGFRis apart from a more frequent appearance of granulomas in AFA-treated patients (Annunziata et al., 2019). These data reinforce the pertinence of AFA as a comprehensive model drug in the study of CADRs.

Besides small-molecule treatments, immunotherapies exist that target the extracellular part of EGFR. Although monoclonal antibodies have shown fewer off-target effects, they can still induce severe skin rashes (Tischer et al., 2017) that are typically associated with activation of immune system components. The involvement of the immune system in the manifestation of at least certain types of CADRs is well-established (Lichtenberger et al., 2013; Mascia et al., 2003). In contrast, KCs harbor EGFR at the cell surface (Peus et al., 1997; Tischer et al., 2017), which could be a target for EGFRis directly affecting KC behavior. In a previous study (Joly-Tonetti et al., 2021), we demonstrated that this drug family directly impacts skin barrier function independent of the immune system. Here, we attempted to identify the biochemical pathway(s) involved, resulting in the direct drug-induced effects on epidermal physiology. To study the direct effects of oncology therapy on epidermal physiology and its consequences on skin barrier function, in our model, we intentionally removed effects related to an overactivated immune system.

Moreover, to better focus on the effects of AFA besides its known action as an EGFRi, exogenous EGF was not included in the media. We specifically designed our experiment as such to avoid activation of EGFR. If EGF was included, the well-documented effect of inhibition of the EGFR-dependent pathway by AFA would dominate the observed results and mask alternative pathways activated by AFA.

We intentionally designed the experiments without adding any protein in the media to avoid any potential decrease in drug availability owing to protein binding. In a previous study (Joly-Tonetti et al., 2021), we introduced the concept of using a physiological concentration of the tested drugs in the *in vitro* models, matching the concentration of the free drug fraction that is not bound to plasma proteins (mostly albumin). Many of the studies performed so far used higher concentrations of drugs, which makes the physiological relevance questionable.

Of course, the same conditions, including absence of EGF and protein in the media, were applied both to the AFA-treated cells and the vehicle-treated controls. Maintaining KCs in a proliferative phenotype requires specific cell culture conditions. Any modification to the cellular metabolism rapidly induces KCs to differentiate (Bakondi et al., 2003; Tsuchisaka et al., 2014; Vessey et al., 1995; Zhang et al., 2002). Exposure to AFA may impact epidermal formation through a single or combination of alterations in KC metabolism.

For the experimental design, we focused on a time-dependent response rather a dose-dependent response. In a previous study (Joly-Tonetti et al., 2021), we tested different doses of several EGFRis and VEGFR inhibitors. We showed that AFA at 100 nM is the right condition for demonstrating TKI effects on epidermal physiology for all tested parameters (differentiation and proliferation markers and decline in the skin barrier function as measured by transepidermal water loss in the RHE model). In this study, we focused on a time-dependent analysis to have a better idea of the kinetics of the AFA-induced effects on KCs.

The PI3K/Akt pathway promotes KC senescence and suppresses KC proliferation

After the exposure of KC to AFA, there was a significant increase of activity related to the PI3K/Akt pathway. This was surprising, because this pathway is downstream of EGFR (Figure 4) and is expected to be negatively regulated by an EGFRi.

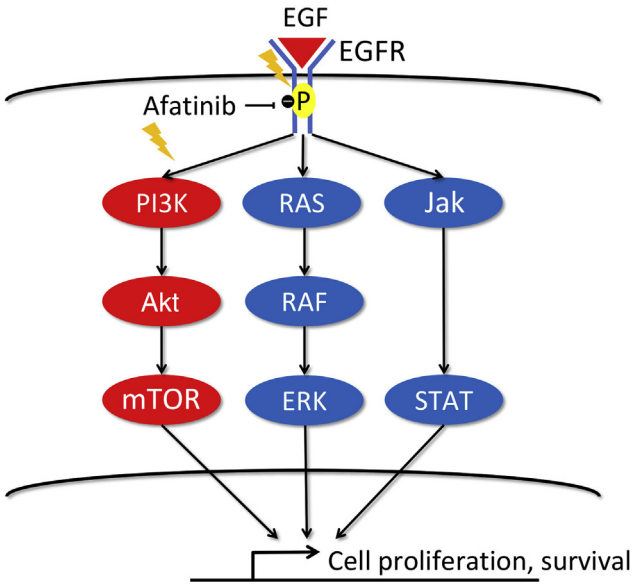

Figure 4. The EGFR signaling pathway and its dependencies. Afatinib inhibits EGFR but activates the PI3K/Akt pathway. EGFR pathway activation triggers three different pathways: PI3K/Akt, RAS/RAF/ERK, and STAT. On AFA treatment of RHE KCs, the PI3K/Akt pathway is alternatively increased. Consequently, genes downstream of the PI3K/Akt pathway involved in proliferation, survival, and senescence were impacted, resulting in skin barrier function impairment. Akt, protein kinase B; ERK, extracellular signal–associated kinase; KC, keratinocyte; PI3K, phosphatidylinositol 3-kinase; RHE, reconstructed human epidermis; STAT, signal transducer and activator of transcription.

Although the PI3K/Akt pathway was upregulated, the RAF/RAS/extracellular signal–associated kinase 1/2 pathway, which is another independent pathway downstream of EGFR activation, was not positively activated after treatment with AFA at 24 hours (Figure 4) (Wee and Wang, 2017). The phosphorylation of Raf1 (phospho-Ser338) and eIF4E (phospho-Ser209) were decreased, and the phosphorylation of Raf1 (phospho-Tyr341), MAPK/extracellular signal–associated kinase 1 (phospho-Ser221), and MAPK/extracellular signal–associated kinase 1 (phospho-Ser217) were not impacted (Supplementary Table S1). These results showed the expected effect of AFA downstream of EGFR. We hypothesize that PI3K/Akt activation was the consequence of an alternative mechanism.

The PI3K/Akt pathway impacts KC gene expression related to cell growth, cell differentiation, senescence and apoptosis, and increased oxidative stress leading to differentiation. AFA impacts skin barrier formation by inducing inflammation and decreasing the innate immune response (Calautti et al., 2005; Janes et al., 2009). Our results showed that the senescence pathway (Figure 1d) was specifically activated through the involvement of PUK, C-Myc, p53, and mTOR proteins. Increased activity in the regulation of these proteins is known to directly induce cell cycle arrest and promote senescence (Demidenko et al., 2010; Iglesias-Bartolome et al., 2012).

We previously reported that the expression of epidermal differentiation markers was increased after AFA exposure (Joly-Tonetti et al., 2021). The PI3K/Akt pathway regulates the increase of filaggrin, loricrin, and cadherin-associated catenin (Calautti et al., 2005), which confirms our previous observations.

Moreover, activation of the PI3K/Akt pathway favors a decrease of cell attachment leading to apoptosis (Janes et al., 2009) and results in an increase of differentiation marker expression and, consequently, induction of KC differentiation. Genes associated with terminal differentiation were transiently increased at 24 hours and decreased at 72 hours of exposure to AFA. These results indicate that AFA induces a rapid induction of KC differentiation and could be the consequence of increased activation of PI3K.

In summary, activation of the PI3K/Akt pathway promotes KC differentiation and suppresses KC proliferation. In certain cases, induction of apoptosis could be involved in more severe conditions, such as in hand-foot syndrome.

AFA induces cellular oxidative stress, which triggers KC differentiation

On exposure to AFA, the expression pattern of several proteins downstream of Akt was altered, including decreased FOXO3A expression, a protein known to be directly downregulated by Akt (Brunet et al., 1999), and consequently increased expression of CDKN1, which is linked to oxidative stress (Marinkovic et al., 2007).

The p53 protein plays a central role in regulating the KC life cycle; it controls the rate of cell proliferation and favors differentiation over apoptosis. Active p53 triggers expression of well-established prosenescence targets. The p21 protein controls the pathways linked to cellular aging and senescence (Herbig et al., 2003). In this regard, increased p53 levels are able to limit oxidative damage and participate in pro-apoptotic and prosenescent activities (Rufini et al., 2013). Nevertheless, our phospho-antibody microarray results do not show an increase in caspase 3 activity (Supplementary Table S1) at any time point, which also confirms our previous results (Joly-Tonetti et al., 2021) that mild to moderate CADRs are not associated with KC apoptosis. However, in more severe conditions such as toxic epidermal necrolysis, p53 activation could be the cause of more serious symptoms (Ido et al., 2012).

EGFRi impact VD3 metabolism in KC

In the presence of EGF, AFA irreversibly inhibits EGFR intracellular signaling by covalently binding to Cys797 of EGFR, Cys805 of HER2, and Cys803 of ErbB-4 (Solca et al., 2012). An off-target activity of the drug has already been demonstrated through nonspecific covalent binding (such as to cyclin-dependent kinase complexes) leading to disturbance of cellular processes (Klaeger et al., 2017). These results suggest that covalent kinase inhibitors have the potential to cross-react, either specifically or nonspecifically, with proteins outside their kinome. Such activity complicates the assignment of biological functions to kinases in chemical biology experiments and could lead to unanticipated toxicities by triggering apoptosis and/or senescence (Lanning et al., 2014). Off-target binding of TKI has been shown to enhance calcium metabolism and contribute to KC differentiation (Kroschwald et al., 2018).

A parallel activation of VD3 metabolism may consequently interfere with extracellular calcium levels to induce KC differentiation (Teichert and Bikle, 2011). A recent study (Shaurova et al., 2020) has shown a direct impact of EGFRi on 1,25-dihydroxyVD3 (1,25(OH)2D3), which is a VD3 metabolite involved in epithelial differentiation.

Our results show that, following AFA exposure, the expression of several CYPs was altered. These include CYP27A1, involved in VD3 metabolism and the degradation of cholesterol to bile acids in both the classic and acidic pathways. A previous study (Kroschwald et al., 2018) has shown that TKIs directly modulate CYP24A1 activity. As a consequence, a change in calcium metabolism takes place that could impact KC differentiation (Elsholz et al., 2014).

Moreover, low levels of a key vitamin D–catabolizing enzyme 24-hydroxylase has been correlated with *CYP24A1* gene expression (Shaurova et al., 2020). Our results show an increase in long noncoding–*CYP24A1* and consequently suggest a decrease in *CYP24A1* expression. Both of these CYPs have been shown to induce calcium metabolism modification (Dinour et al., 2013). Furthermore, 1,25(OH)2VD3 induced transcriptional responses, including increased mRNA levels of *CYP24A1*, a well-characterized direct target of the vitamin D receptor (Shaurova et al., 2020). All together, these results showed enhanced expression of 1,25(OH)2VD3 associated with an upregulation of *CYP24A1*, both of which promote epithelial differentiation.

It is known that 1,25(OH)2VD3 induces transcription of multiple cell adhesion molecules (Pálmer et al., 2001), which confirms our previous results showing that AFA affects epidermal size and volume and increases the expression of differentiation markers (involucrin, desmoglein, and filaggrin)

(Joly-Tonetti et al., 2021). In relation to oxidative stress, VD3 is known to be a potent inducer of MT, able to capture harmful oxidants, such as the superoxide and hydroxyl radicals (Nzengue et al., 2008) (Figure 3b). MT may act as a radical scavenger in oxygen-mediated CYP activity.

Studies have demonstrated that deregulation of the PI3K/Akt pathway synergizes with antiproliferative signaling of VD3 to induce cell senescence (Axanova et al., 2010; da Silva Teixeira et al., 2020) and confirmed both the involvement of VD3 and the senescence pathway as potential mechanisms of CADRs.

TKIs in general, and specifically AFA, are known to induce photosensitivity (Dai et al., 2017). It is very likely that exposure to solar UVR may interact with such therapies affecting VD3 metabolism and relating to increased skin photosensitivity.

Immune alterations after EGFRi treatment compromise skin barrier protection

The mechanisms through which the immune response is affected by TKI therapy are still poorly understood. In this work, protein and gene expression assays demonstrated involvement of the Th2 response as a result of a combined increase of related *IL4* and *IL13* gene expression and a decrease of both the Th1 response and the innate immune response via S100 proteins and the inflammasome. Th2 cytokine expression also contributes to decreased expression of S100 proteins, which are involved in the regulation of proliferation, differentiation, apoptosis, calcium ion homeostasis, energy metabolism, inflammation, and migration/invasion, through interactions with a variety of target proteins, including enzymes, cytoskeletal subunits, receptors, transcription factors, and nucleic acids (Howell et al., 2008). The same changes are observed in atopic dermatitis, leading to intense pruritis, dryness, and erythema in localized lesions (Bieber, 2008). Moreover, a dysregulated VD3 metabolism negatively impacts the immune response in KCs (Kroschwald et al., 2018).

In this work, we demonstrated the mechanism of direct action of AFA, an EGFRi, on KC biology. This could be one of several mechanisms of oncology-related CADRs. The specific pathology of acneiform folliculitis, one of the common CADRs, remains unknown. The AFA-induced effects on KCs and the resulting reduced barrier function (Joly-Tonetti et al., 2021) could be one of the involved mechanisms. It is interesting to note that primary skin reaction to EGFRis is an acneiform folliculitis that also has shown to be related to a weakening of skin barrier function (Meyer et al., 2015; Yamamoto et al., 1995). In the case of acneiform folliculitis, because the skin irritation is localized around hair follicle structures, one could hypothesize that beyond the effect on the skin barrier, there can be other contributing factors: (i) EGFRi targeting hair follicle cells (including stem cells in the bulge or the papilla), (ii) immune cell activation and targeting of follicular papilla, (iii) microbiome involvement (*Cutibacterium acnes*), (iv) involvement of sebaceous glands, and so on.

Impaired epidermal function associated with impaired innate immune response increases the susceptibility of individuals to recurrent bacterial and viral skin infections that are often clinically observed. Use of tetracycline to compensate for the impaired innate immune response after AFA exposure has shown improvement of CADR symptoms (Arrieta et al., 2015).

These markers could be useful in designing better strategies for prevention of skin damage resulting from oncology therapies.

To conclude, this work demonstrates that the PI3K/Akt pathway plays a pivotal role in the pathogenesis of CADRs by quickly driving KC differentiation. This mechanism could explain the manifestation of CADR symptoms and also indicate that VD3 plays an important role in CADRs, TKIs are known to impact VD3 metabolism. A deregulated VD3 pathway impacts KC differentiation through alterations in intracellular calcium activity, increased differentiation protein expression, decreased innate response, and an overexpression of CYP21A1. Taken together, these results bring molecular insights in the mechanisms of CADRs that can be useful in clinical diagnosis and assessment of the efficacy of a CADR treatment protocol.

MATERIALS AND METHODS

Drug preparation

The AFA concentration used in the experiments was selected at a subcytotoxic level of 100 nM, as previously reported (Joly-Tonetti et al., 2021). AFA was purchased from Caymanchem (Ann Arbor, MI) and was prepared from a 10 mM stock solution dissolved in DMSO (Sigma-Aldrich Chimie, St. Quentin Fallavier, France). Consequently, the final DMSO concentration was 0.001% for 100 nM. The control was composed of the same DMSO volume as the AFA solution.

RHE model

Large 4 cm^2 RHEs were purchased from Episkin (Lyon, France) and were cultured for 24 hours without EGF before exposure to AFA. RHE treatment was performed in Epilife medium without EGF and without proteins (MEPI500CA, Thermo Fisher Scientific, Waltham, MA). Short, intermediate, and long drug exposure times were selected of 20 minutes, 24 hours, and 72 hours, respectively, for the protein phosphorylation assay and 6 hours, 24 hours, and 72 hours, respectively, for the gene profiling assay. Quadruplicate repeats were performed for all timepoints and conditions.

Antibody microarrays for protein phosphorylation and expression profiling

The Phospho Explorer Antibody Array (Full Moon BioSystems, Sunnyvale, CA) was performed by TebuBio (Le Perray-en-Yvelines, France) using 1,330 duplicate spots matching 1,318 proteins (phosphorylated and unphosphorylated), housekeeping proteins (β-actin, GAPDH), negative controls (n = 4), empty spots (n = 4), and positive markers (n = 2). Briefly, RHEs were washed in cold PBS and directly stored at −80 °C. The samples were treated following the manufacturer's protocol. Sample volumes of 60 μg were incubated with biotin for 2 hours followed by 30-minute incubation in the Stop reagent (Full Moon BioSystems, Sunnyvale, CA). Membranes containing printed antibodies were blocked for 40 minutes with the blocking reagent under agitation, and then they were washed and incubated in a coupling chamber for 2 hours. After sample removing and three successive washes, the detection step was performed after addition of 30 μl of cyanine 3-streptavidin (1 mg/ml) for 20 minutes incubation at room temperature in the dark. The slide was then

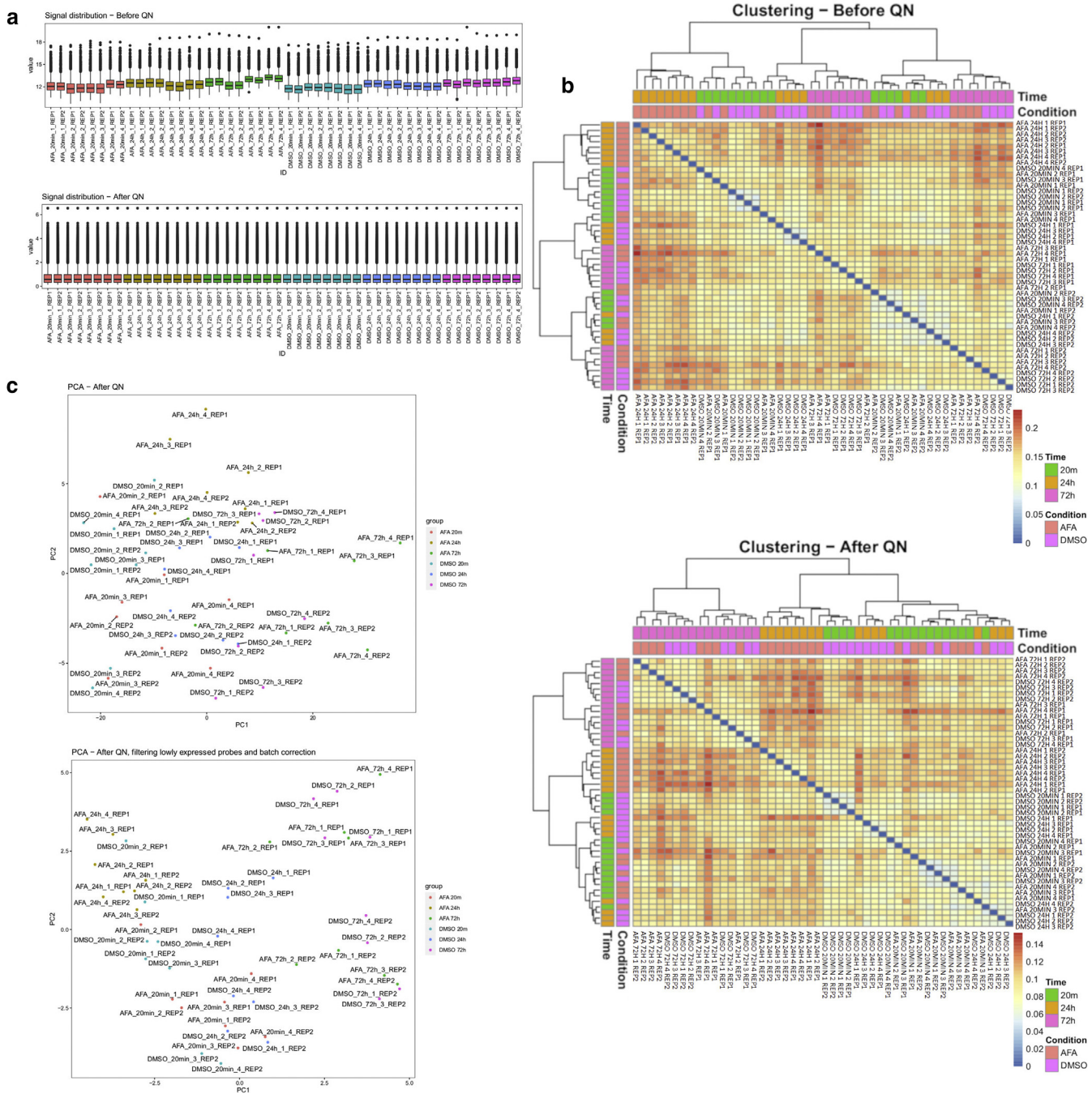

Figure 5. Protein array quality check before and after normalization and filtering. (**a**) Box plot depicting the distribution of fluorescence signal before and after QN for the phospho-antibody microarray. (**b**) Unsupervised biclustering for the phosphorylation protein array before and after QN (distance: Pearson's correlation, aggregation criterion = Ward's D2). (**c**) Biplots for PCA, before normalization and after normalization and debatching for the phosphorylation protein array. QN followed by the debatching step allows for the capture of time along PC1 and treatment along PC2. AFA, afatinib; h, hour; ID, identification; min, minute; PC, principal component; PCA, principal component analysis; QN, quantile normalization.

washed, dried by centrifugation, and scanned on a microarray scanner (Innopsys Innoscan 710).

Gene expression profiling

Transcriptomic analysis was performed by Genex (Longjumeau, France). RHEs were removed from their supporting polycarbonate membrane and immediately transferred to RLT buffer (Qiagen, Hilden, Germany) containing 1% β-mercaptoethanol. Polycarbonate membranes were scraped to remove attached remained basal cells and transferred to corresponding vials containing RHEs. Samples were immediately stored at −80 °C.

Total RNA, including microRNA, was extracted using AllPrep DNA/RNA/miRNA Universal kit from Qiagen. RNA quality was assessed by Experion (Bio-Rad, Marnes-la-Coquette, France). All RNA quality indicators were above 7. A quantity of 100 ng of total RNA was transcribed and stained with cyanine 3 using RNA Low Input Quick Amp Labeling Kit One Color (Agilent Technologies, Les Ulis, France) according to the manufacturer's

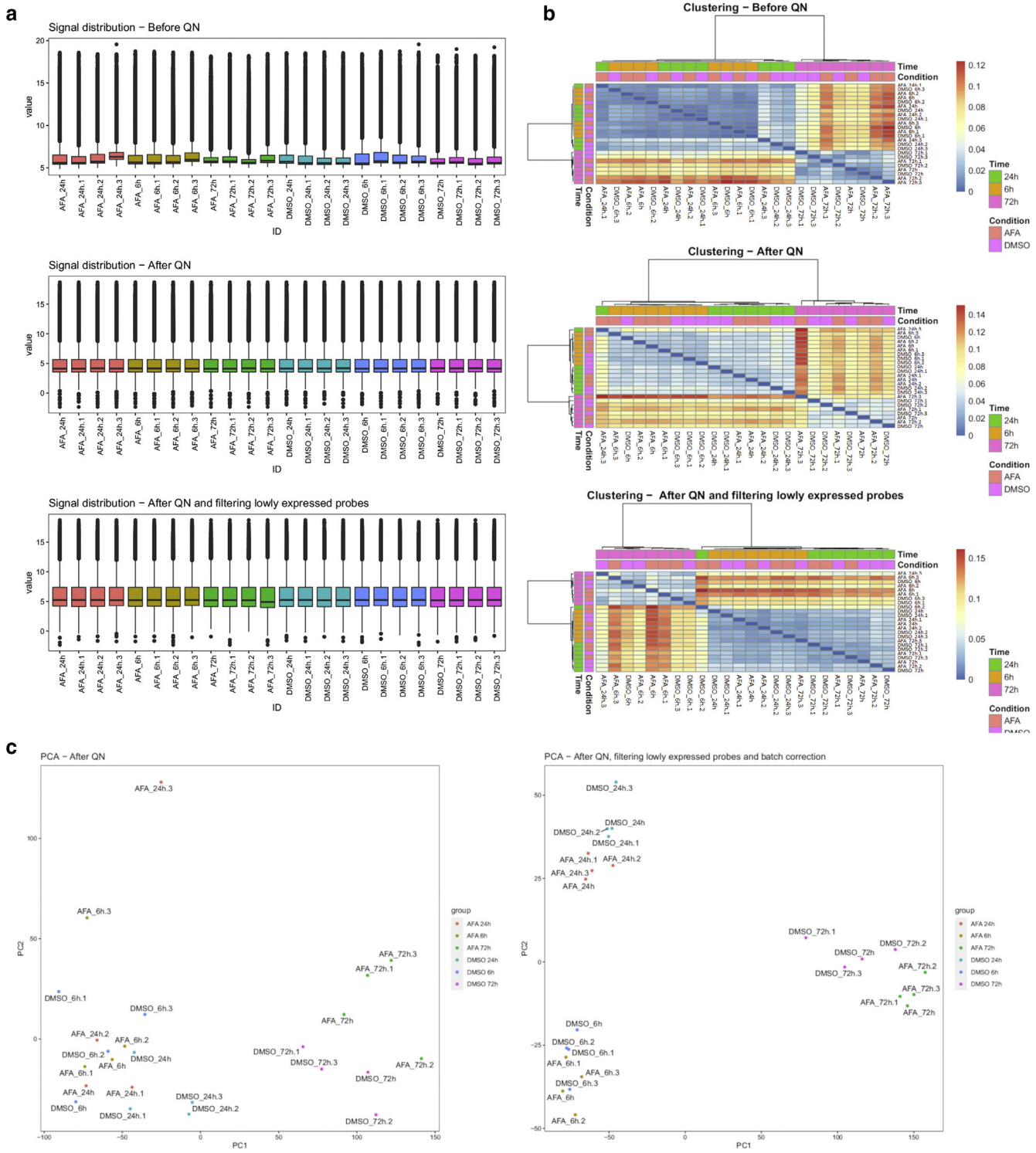

Figure 6. Transcriptome quality check before and after normalization and filtering. (**a**) Box plot depicting the distribution of fluorescence signal before normalization, after QN, and after QN and debatching for the transcriptomic assay. (**b**) Unsupervised biclustering for the transcriptome assay before normalization, after QN, and after QN and debatching (distance: Pearson's correlation, aggregation criterion = Ward's D2). (**c**) Biplots for PCAs before normalization and after normalization and debatching for the transcriptome assay. QN followed by the debatching step allows for the capture of time along PC1 and treatment along PC2. AFA, afatinib; h, hour; ID, identification; PC, principal component; PCA, principal component analysis; QN, quantile normalization.

instructions. All specific activity was above 6 pmol cyanine 3 per μg complementary RNA and the yield above 1.65 μg. An equal amount (600 ng) of cyanine 3–labeled complementary RNA was fragmented and subsequently hybridized for 17 hours at 65 °C onto human SurePrint 8x60K version 3 microarray (Agilent Technologies). The microarrays were then washed and scanned according to the manufacturer's instructions by Scanner G2505C (Agilent Technologies). Gene expression data were further processed using Feature Extraction (version 10.7) software.

Data processing

For both protein phosphorylation and transcriptome array data, a background correction followed by a quantile normalization was performed using the RMA framework as implemented in the limma package. This procedure is aimed at normalizing the median expression between arrays (Figures 5 and 6).

Quality check was performed to properly evaluate the impact of the quantile normalization and filtering using a graphical data visualization before and after normalization, associated with box plot, unsupervised clustering, principal component analysis, and multidimensional scaling (Figures 5 and 6).

Volcano plots were determined based on a significant differential expression of $-\log_{10}$ of transformed q-values after applying a 10% false discovery rate followed by the Benjamini-Hochberg post-analysis (y-axis). The x-axis indicates the difference between the two groups (AFA vs. control). Protein phosphorylation and gene expression values were $\log_2$ transformed to ensure normal distribution.

To identify the phosphorylation sites and genes impacted by AFA at any time point, a differential analysis relying on the general linear model was performed, considering time and treatment interaction, using the limma package.

Gene and protein set enrichment analyses were then performed to identify classes of genes or proteins that are over-represented in genes sets that are upregulated or downregulated and may have an association with disease phenotypes. The Kyoto Encyclopedia of Genes and Genomes pathway analysis was performed based on the set enrichment analysis with significant altered phosphorylation sites and gene expression with $P < 0.05$ to establish the main affected pathway.

Data availability statement

Microarray data are publicly available from the Gene Expression Omnibus database (https://www.ncbi.nlm.nih.gov/geo; GSE167246).

SUPPLEMENTARY MATERIAL

Supplementary material is linked to the online version of the paper at www.jidonline.org, and at https://doi.org/10.1016/j.xjidi.2021.100009.

ORCIDs

Thomas Ondet: http://orcid.org/0000-0001-8888-9884
Pierre-François Roux: http://orcid.org/0000-0002-0695-4206
Mario Monshouwer: http://orcid.org/0000-0001-9605-4692
Georgios N. Stamatas: http://orcid.org/0000-0003-4544-7597

AUTHOR CONTRIBUTIONS

Conceptualization: GNS, MM; Data Curation: TO, PFR; Formal Analysis: GNS, TO, PFR; Funding Acquisition: GNS, MM; Investigation: GNS, MM, TO; Methodology: GNS, TO, PFR; Project Administration: TO, GNS, MM; Resources: GNS, MM, TO, PFR; Supervision: GNS, MM; Writing - Original Draft Preparation: TO, PFR, GNS; Writing - Review and Editing: TO, PFR, GNS, MM

ACKNOWLEDGMENTS

This study was sponsored in full by Janssen and Johnson & Johnson Company. We thank Angel Patatian from Genex company (Longjumeau, France) for their participation to the conception and experiment realization of the transcriptomic data. We thank Eric Mennesson and Joffrey Guillier from Tebu Bio (Le Perray-en-Yvelines, France) for their participation in the conception and experiment realization of the protein phosphorylation assays.

CONFLICT OF INTEREST

GNS, PFR, and TO are employees of Johnson & Johnson Santé Beauté France, a manufacturer of skin care products. MM is an employee of Janssen pharmaceutical company. The authors of the manuscript declare no competing commercial/financial interests.

REFERENCES

Ali R, Brown W, Purdy SC, Davisson VJ, Wendt MK. Biased signaling downstream of epidermal growth factor receptor regulates proliferative versus apoptotic response to ligand. Cell Death Dis 2018;9:976.

Annunziata MC, Ferrillo M, Cinelli E, Panariello L, Rocco D, Fabbrocini G. Retrospective analysis of skin toxicity in patients under anti-EGFR tyrosine kinase inhibitors: our experience in lung cancer. Open Access Maced J Med Sci 2019;7:973–7.

Arrieta O, Vega-González MT, López-Macías D, Martínez-Hernández JN, Bacon-Fonseca L, Macedo-Pérez EO, et al. Randomized, open-label trial evaluating the preventive effect of tetracycline on afatinib induced-skin toxicities in non-small cell lung cancer patients. Lung Cancer 2015;88:282–8.

Axanova LS, Chen YQ, McCoy T, Sui G, Cramer SD. 1,25-dihydroxyvitamin D3 and PI3K/AKT inhibitors synergistically inhibit growth and induce senescence in prostate cancer cells. Prostate 2010;70:1658–71.

Bakondi E, Gönczi M, Szabó E, Bai P, Pacher P, Gergely P, et al. Role of intracellular calcium mobilization and cell-density-dependent signaling in oxidative-stress-induced cytotoxicity in HaCaT keratinocytes. J Invest Dermatol 2003;121:88–95.

Bieber T. Atopic dermatitis. N Engl J Med 2008;358:1483–94.

Brunet A, Bonni A, Zigmond MJ, Lin MZ, Juo P, Hu LS, et al. Akt promotes cell survival by phosphorylating and inhibiting a Forkhead transcription factor. Cell 1999;96:857–68.

Calautti E, Li J, Saoncella S, Brissette JL, Goetinck PF. Phosphoinositide 3-kinase signaling to Akt promotes keratinocyte differentiation versus death. J Biol Chem 2005;280:32856–65.

Cheng JB, Levine MA, Bell NH, Mangelsdorf DJ, Russell DW. Genetic evidence that the human CYP2R1 enzyme is a key vitamin D 25-hydroxylase. Proc Natl Acad Sci USA 2004;101:7711–5.

da Silva Teixeira S, Harrison K, Uzodike M, Rajapakshe K, Coarfa C, He Y, et al. Vitamin D actions in neurons require the PI3K pathway for both enhancing insulin signaling and rapid depolarizing effects. J Steroid Biochem Mol Biol 2020;200:105690.

Dai J, Belum VR, Wu S, Sibaud V, Lacouture ME. Pigmentary changes in patients treated with targeted anticancer agents: a systematic review and meta-analysis. J Am Acad Dermatol 2017;77:902–10.e2.

Demidenko ZN, Korotchkina LG, Gudkov AV, Blagosklonny MV. Paradoxical suppression of cellular senescence by p53. Proc Natl Acad Sci USA 2010;107:9660–4.

Dinour D, Beckerman P, Ganon L, Tordjman K, Eisenstein Z, Holtzman EJ. Loss-of-function mutations of CYP24A1, the vitamin D 24-hydroxylase gene, cause long-standing hypercalciuric nephrolithiasis and nephrocalcinosis. J Urol 2013;190:552–7.

Eckert RL, Efimova T, Dashti SR, Balasubramanian S, Deucher A, Crish JF, et al. Keratinocyte survival, differentiation, and death: many roads lead to mitogen-activated protein kinase. J Investig Dermatol Symp Proc 2002;7:36–40.

Elsholz F, Harteneck C, Muller W, Friedland K. Calcium–a central regulator of keratinocyte differentiation in health and disease. Eur J Dermatol 2014;24:650–61.

Herbig U, Wei W, Dutriaux A, Jobling WA, Sedivy JM. Real-time imaging of transcriptional activation in live cells reveals rapid up-regulation of the cyclin-dependent kinase inhibitor gene CDKN1A in replicative cellular senescence. Aging Cell 2003;2:295–304.

Howell MD, Fairchild HR, Kim BE, Bin L, Boguniewicz M, Redzic JS, et al. Th2 cytokines act on S100/A11 to downregulate keratinocyte differentiation. J Invest Dermatol 2008;128:2248–58.

Ido T, Kiyohara T, Takahashi H, Yamaguchi Y, Tani D, Kumakiri M. Toxic epidermal necrolysis following allergic contact dermatitis caused by occupational exposure to ultraviolet-cured inks. Acta Derm Venereol 2012;92:313–5.

Iglesias-Bartolome R, Patel V, Cotrim A, Leelahavanichkul K, Molinolo AA, Mitchell JB, et al. mTOR inhibition prevents epithelial stem cell senescence and protects from radiation-induced mucositis. Cell Stem Cell 2012;11:401–14.

Janes SM, Ofstad TA, Campbell DH, Eddaoudi A, Warnes G, Davies D, et al. PI3-kinase-dependent activation of apoptotic machinery occurs on

commitment of epidermal keratinocytes to terminal differentiation. Cell Res 2009;19:328–39.

Jänicke RU, Sprengart ML, Wati MR, Porter AG. Caspase-3 is required for DNA fragmentation and morphological changes associated with apoptosis. J Biol Chem 1998;273:9357–60.

Joly-Tonetti N, Ondet T, Monshouwer M, Stamatas GN. EGFR inhibitors switch keratinocytes from a proliferative to a differentiative phenotype affecting epidermal development and barrier function. BMC Cancer 2021;21:5.

Klaeger S, Heinzlmeir S, Wilhelm M, Polzer H, Vick B, Koenig PA, et al. The target landscape of clinical kinase drugs. Science 2017;358:eaan4368.

Kroschwald L, Suttorp M, Tabeatauer J, Zimmermann N, Günther C, Bauer A. Off-target effect of imatinib and nilotinib on human vitamin D3 metabolism. Mol Med Rep 2018;17:1382–8.

Lacouture ME. Mechanisms of cutaneous toxicities to EGFR inhibitors. Nat Rev Cancer 2006;6:803–12.

Lanning BR, Whitby LR, Dix MM, Douhan J, Gilbert AM, Hett EC, et al. A road map to evaluate the proteome-wide selectivity of covalent kinase inhibitors. Nat Chem Biol 2014;10:760–7.

Li D, Ambrogio L, Shimamura T, Kubo S, Takahashi M, Chirieac LR, et al. BIBW2992, an irreversible EGFR/HER2 inhibitor highly effective in preclinical lung cancer models. Oncogene 2008;27:4702–11.

Lichtenberger BM, Gerber PA, Holcmann M, Buhren BA, Amberg N, Smolle V, et al. Epidermal EGFR controls cutaneous host defense and prevents inflammation. Sci Transl Med 2013;5:199ra111.

Lippens S, Denecker G, Ovaere P, Vandenabeele P, Declercq W. Death penalty for keratinocytes: apoptosis versus cornification. Cell Death Differ 2005;12(Suppl. 2):1497–508.

Marinkovic D, Zhang X, Yalcin S, Luciano JP, Brugnara C, Huber T, et al. Foxo3 is required for the regulation of oxidative stress in erythropoiesis. J Clin Invest 2007;117:2133–44.

Mascia F, Mariani V, Girolomoni G, Pastore S. Blockade of the EGF receptor induces a deranged chemokine expression in keratinocytes leading to enhanced skin inflammation. Am J Pathol 2003;163:303–12.

Mehlig LM, Garve C, Tauer JT, Suttorp M, Bauer A. Inhibitory effects of imatinib on vitamin D3 synthesis in human keratinocytes. Mol Med Rep 2015;11:3143–7.

Meyer K, Pappas A, Dunn K, Cula GO, Seo I, Ruvolo E, et al. Evaluation of seasonal changes in facial skin with and without acne. J Drugs Dermatol 2015;14:593–601.

Missero C, Di Cunto F, Kiyokawa H, Koff A, Dotto GP. The absence of p21(Cip1/WAF1) alters keratinocyte growth and differentiation and promotes ras-tumor progression. Genes Dev 1996;10:3065–75.

Norlin M, Von Bahr S, Björkhem I, Wikvall K. On the substrate specificity of human CYP27A1: implications for bile acid and cholestanol formation. J Lipid Res 2003;44:1515–22.

Nzengue Y, Steiman R, Garrel C, Lefèbvre E, Guiraud P. Oxidative stress and DNA damage induced by cadmium in the human keratinocyte HaCaT cell line: role of glutathione in the resistance to cadmium. Toxicology 2008;243:193–206.

Pálmer HG, González-Sancho JM, Espada J, Berciano MT, Puig I, Baulida J, et al. Vitamin D(3) promotes the differentiation of colon carcinoma cells by the induction of E-cadherin and the inhibition of beta-catenin signaling. J Cell Biol 2001;154:369–87.

Peus D, Hamacher L, Pittelkow MR. EGF-receptor tyrosine kinase inhibition induces keratinocyte growth arrest and terminal differentiation. J Invest Dermatol 1997;109:751–6.

Rufini A, Tucci P, Celardo I, Melino G. Senescence and aging: the critical roles of p53. Oncogene 2013;32:5129–43.

Shaurova T, Dy GK, Battaglia S, Hutson A, Zhang L, Zhang Y, et al. Vitamin D3 metabolites demonstrate prognostic value in EGFR-mutant lung adenocarcinoma and can be deployed to oppose acquired therapeutic resistance. Cancers (Basel) 2020;12:675.

Solca F, Dahl G, Zoephel A, Bader G, Sanderson M, Klein C, et al. Target binding properties and cellular activity of afatinib (BIBW 2992), an irreversible ErbB family blocker. J Pharmacol Exp Ther 2012;343:342–50.

Teichert A, Bikle DD. Regulation of keratinocyte differentiation by vitamin D and its relationship to squamous cell carcinoma. In: Glick A, Waes C, editors. Signaling Pathways in Squamous Cancer. New York: Springer; 2011. p. 283–303.

Tischer B, Huber R, Kraemer M, Lacouture ME. Dermatologic events from EGFR inhibitors: the issue of the missing patient voice. Support Care Cancer 2017;25:651–60.

Tsuchisaka A, Furumura M, Hashimoto T. Cytokine regulation during epidermal differentiation and barrier formation. J Invest Dermatol 2014;134:1194–6.

Vessey DA, Lee KH, Boyer TD. Differentiation-induced enhancement of the ability of cultured human keratinocytes to suppress oxidative stress. J Invest Dermatol 1995;104:355–8.

Vivanco I, Sawyers CL. The phosphatidylinositol 3-kinase–AKT pathway in human cancer. Nat Rev Cancer 2002;2:489–501.

Wee P, Wang Z. Epidermal growth factor receptor cell proliferation signaling pathways. Cancers (Basel) 2017;9:52.

Whitman M, Downes CP, Keeler M, Keller T, Cantley L. Type I phosphatidylinositol kinase makes a novel inositol phospholipid, phosphatidylinositol-3-phosphate. Nature 1988;332:644–6.

Yamamoto A, Takenouchi K, Ito M. Impaired water barrier function in acne vulgaris. Arch Dermatol Res 1995;287:214–8.

Zhang T, Woods TL, Elder JT. Differential responses of S100A2 to oxidative stress and increased intracellular calcium in normal, immortalized, and malignant human keratinocytes. J Invest Dermatol 2002;119:1196–201.